



Wind Generation Participation in Power System Frequency Response

Preprint

Vahan Gevorgian and Yingchen Zhang
National Renewable Energy Laboratory

*Presented at the 15th International Workshop on Large-Scale
Integration of Wind Power into Power Systems as well as on
Transmission Networks for Offshore Wind Power Plants
Vienna, Austria
November 15–17, 2016*

**NREL is a national laboratory of the U.S. Department of Energy
Office of Energy Efficiency & Renewable Energy
Operated by the Alliance for Sustainable Energy, LLC**

This report is available at no cost from the National Renewable Energy
Laboratory (NREL) at www.nrel.gov/publications.

Conference Paper
NREL/CP-5D00-67287
January 2017

Contract No. DE-AC36-08GO28308

NOTICE

The submitted manuscript has been offered by an employee of the Alliance for Sustainable Energy, LLC (Alliance), a contractor of the US Government under Contract No. DE-AC36-08GO28308. Accordingly, the US Government and Alliance retain a nonexclusive royalty-free license to publish or reproduce the published form of this contribution, or allow others to do so, for US Government purposes.

This report was prepared as an account of work sponsored by an agency of the United States government. Neither the United States government nor any agency thereof, nor any of their employees, makes any warranty, express or implied, or assumes any legal liability or responsibility for the accuracy, completeness, or usefulness of any information, apparatus, product, or process disclosed, or represents that its use would not infringe privately owned rights. Reference herein to any specific commercial product, process, or service by trade name, trademark, manufacturer, or otherwise does not necessarily constitute or imply its endorsement, recommendation, or favoring by the United States government or any agency thereof. The views and opinions of authors expressed herein do not necessarily state or reflect those of the United States government or any agency thereof.

This report is available at no cost from the National Renewable Energy Laboratory (NREL) at www.nrel.gov/publications.

Available electronically at SciTech Connect <http://www.osti.gov/scitech>

Available for a processing fee to U.S. Department of Energy and its contractors, in paper, from:

U.S. Department of Energy
Office of Scientific and Technical Information
P.O. Box 62
Oak Ridge, TN 37831-0062
OSTI <http://www.osti.gov>
Phone: 865.576.8401
Fax: 865.576.5728
Email: reports@osti.gov

Available for sale to the public, in paper, from:

U.S. Department of Commerce
National Technical Information Service
5301 Shawnee Road
Alexandria, VA 22312
NTIS <http://www.ntis.gov>
Phone: 800.553.6847 or 703.605.6000
Fax: 703.605.6900
Email: orders@ntis.gov

Cover Photos by Dennis Schroeder: (left to right) NREL 26173, NREL 18302, NREL 19758, NREL 29642, NREL 19795.

NREL prints on paper that contains recycled content.

Wind Generation Participation in Power System Frequency Response

Vahan Gevorgian, Yingchen Zhang
National Renewable Energy Laboratory
Golden, CO-80401, USA

Abstract—The electrical frequency of an interconnected power system must be maintained close to its nominal level at all times. Excessive under- and over-frequency excursions can lead to load shedding, instability, machine damage, and even blackouts. There is a rising concern in the electric power industry in recent years about the declining amount of inertia and primary frequency response (PFR) in many interconnections. This decline may continue due to increasing penetrations of inverter-coupled generation and the planned retirements of conventional thermal plants. Inverter-coupled variable wind generation is capable of contributing to PFR and inertia with a response that is different from that of conventional generation. It is not yet entirely understood how such a response will affect the system at different wind power penetration levels. The modeling work presented in this paper evaluates the impact of wind generation’s provision of these active power control strategies on a large, synchronous interconnection. All simulations were conducted on the U.S. Western Interconnection with different levels of instantaneous wind power penetrations (up to 80%). The ability of wind power plants to provide PFR—and a combination of synthetic inertial response and PFR—significantly improved the frequency response performance of the system.

Keywords - *interconnection frequency response; inertia; primary frequency response.*

I. INTRODUCTION

The ability of a power system to maintain its electrical frequency within a safe range is crucial for stability and reliability. Frequency response is a measure of an interconnection’s ability to stabilize the frequency immediately following the sudden loss of generation or load. An interconnected power system must have adequate resources to respond to a *variety of contingency events to ensure rapid restoration of the balance between generation and load*. Primary frequency response (PFR)—also called primary control reserve [1] and frequency responsive reserve [2]—is the capacity available for automatic local response to frequency excursions through turbine speed governors and frequency responsive demand that adjusts to counter-frequency deviations to stabilize the system. System inertia is the cumulative synchronous generation and load inertia that injects or extracts stored kinetic energy from the rotating mass of the machine and slows the speed of the frequency deviation. The combined response of PFR and inertia is essential to arrest electrical frequency changes before they trigger underfrequency load-shedding (UFLS)

relays, generation protection relays, machine damage, or reach unstable levels that could potentially lead to a blackout.

Frequency response is typically measured in MW/0.1 Hz, which is the response given with the steady-state frequency deviation. Other metrics have been proposed recently that focus more on the frequency nadir [3]. The frequency response of a power system with high levels of variable generation to sudden large imbalances between generation and load has been the focal point of many studies both nationally and internationally [3]–[5]. Currently, variable energy resources rarely provide PFR. Because they are not synchronous to the grid, they also do not contribute to system inertia. Lower system inertia as a result of increased renewable penetration will cause increased rates of change of frequency immediately following a disturbance. Lower amounts of PFR as a result of the displacement of conventional generators by variable generation will cause greater steady-state frequency deviations.

In the United States, recent studies have shown that frequency response has been declining during the last several years [6], [7]. Physical reasons for this include excessive governor dead bands, generators that operate in modes that do not offer PFR (e.g., sliding-pressure mode), and blocked governors [8], [9]. Other reasons may be institutional [10] or caused by a lack of incentives in electricity market designs [11], [24]. Such declines may translate to a decrease in bulk power system reliability. In particular, the response of the U.S. Eastern Interconnection of the United States and Canada has been steadily declining by approximately 60 MW/0.1 Hz to 70 MW/0.1Hz per year during the past two decades [7]. However, frequency response should not be compared among interconnections because the characteristics of the interconnections differ significantly (e.g., number of thermal and hydro units, transmission distances, operational practices, and load profiles). The chart in Figure 1 shows the frequency response of 66 events in the U.S. Western Interconnection during 2012–2014 [8]. A simple linear regression model was used to describe the relationship between time and frequency response. It indicates a small negative slope, meaning that the frequency response variable has a slow decreasing general trend in time. This can be caused by many factors, not necessarily by increasing penetrations of wind and solar generation.

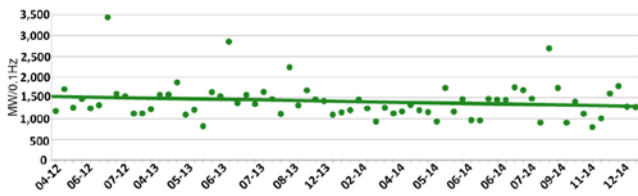


Figure 1. U.S. Western Interconnection frequency response

A recent study [9] indicated that adequate frequency response in the Western Interconnection can be maintained for conditions of high levels of wind and solar penetration if frequency-responsive controls on wind and solar power plants and energy storage are used.

An IEEE task force report studied this issue with great detail and developed a number of conclusions and recommendations, including those on the importance of wind generation to provide PFR to prevent future declines in the frequency response of U.S. interconnections [12]. These concerns prompted further industrywide efforts by the North American Electric Reliability Corporation and regional reliability entities to broaden understanding and increase transparency by highlighting mitigation efforts to ensure adequate frequency response. The Federal Energy Regulatory Commission's (FERC's) Frequency Response Initiative sets a number of objectives to comprehensively address the issues related to frequency response [13]. These objectives include (a) a clearer identification of frequency-related reliability factors; (b) improvements in frequency response metrics; and (c) assessing the impacts of emerging technologies, including inverter-coupled renewable energy generation. The proposed BAL-003-1 standard would set a minimum frequency response obligation for balancing authorities within an interconnection and means for measuring their performance [14]. It requires sufficient frequency response from a balancing authority area to maintain interconnection frequency within predefined bounds. A systematic approach to identifying the frequency response that is useful for operating a reliable system with increased amounts of variable renewable generation was presented in [15]. It also confirmed the validity of using frequency response as a predictive metric to assess the reliable operation of interconnected systems.

Although some studies have been performed with detailed simulations on how increased penetrations of wind power may affect the frequency response of the system, few have gone into the level of detail needed to understand the effects that different wind controls have on a large system with various sensitivities. Many researchers and wind turbine manufacturers have proposed different designs that allow wind power plants to provide capabilities similar to PFR and inertial control [15]. The benefits and drawbacks of inertial and PFR controls by wind power in an island power system were analyzed in [16]. Another study looked at the impacts of wind PFR on the frequency response of the Eastern Interconnection [17]. It demonstrated that adequate frequency response of the Eastern Interconnection can be achieved at high levels of wind power penetration by employing both inertial and PFR controls for wind power.

This study focuses on investigating the performance of the Western Interconnection under various wind power penetration scenarios. We described the initial findings of this work in [18] and [19], in which we investigated the impacts of wind power providing inertial and PFR

separately. This paper provides a further in-depth analysis of the system-level frequency response at higher wind power penetrations and various levels of enabled governors in the conventional fleet. The major contribution of this work is that it is the first attempt to investigate the frequency response of an entire interconnection at very high levels of instantaneous wind power penetration (up to 80% of the load) as well as the grid performance when wind power provides frequency support under such high penetrations. It is also the first analysis of PFR of the interconnection using the latest FERC frequency response metrics described in [14].

This work uses many methods and assumptions used in a similar simulation study [20]. Section II of this paper gives an overview of the frequency response metrics used in the study. Section III provides an overview of the system and assumptions used in the study. Section IV provides results of different active power control strategies from different penetration levels of wind. Section V concludes. More in-depth analysis is presented by the same authors in [21].

II. FREQUENCY RESPONSE METRICS

In this work, we adopted a similar approach to frequency response metrics as that described in [3]. We turned to a description of a real frequency event that took place in the Western Interconnection on August 6, 2011, and was recorded by the National Renewable Energy Laboratory (NREL) frequency monitoring system. This event started after a large generation loss at $t=0$ s, as shown in Figure 2. The Point A value was the predisturbance frequency, and it was calculated as an average of frequency values from $t=0$ to $t=-16$ s [14]. The grid frequency started declining immediately because of an imbalance between generation and load. The initial rate of change of frequency was approximately -63 mHz/s, and this was determined by the amount of the rotating mass on the interconnection. The PFR from conventional generation started to respond immediately after the frequency decline passed beyond their governor dead-band thresholds. The characteristics of the system inertia and PFR determine the lowest frequency (nadir), which is shown as Point C in Figure 2.

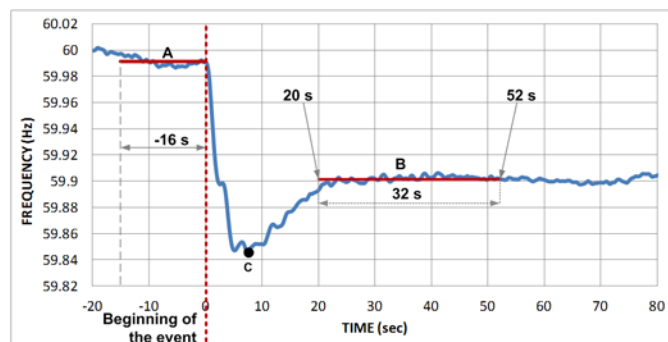


Figure 2. Description of BAL-003-1 frequency response metrics

Important characteristics are the system inertia, amount of PFR headroom, and the response speed of PFR. Point C needs to be higher than the highest set point for the UFLS within an interconnection. Measuring the level of Point C based on the large credible disturbances the interconnection plans for helps determine the amount and characteristics of PFR that are needed to arrest the frequency decline above the UFLS settings. After the frequency decline has been

arrested, continued delivery of PFR will stabilize the frequency to a steady state (Point B). The point at which the frequency is stabilized is often referred to as steady-state frequency. The B value is determined by averaging the frequency values from a period of 32 s starting at $t=20$ s after the disturbance [14].

The Union for the Coordination of the Transmission of Electricity Policy 1 in Europe set requirement metrics for primary frequency control on permissible frequency variations and minimum and maximum instantaneous frequency after the loss of generation or load. Other requirements include frequency dead band, deployment times, and duration of the response by participating control areas [1].

The work presented in this paper focused on assessing the impact of wind generation on the frequency response of the Western Interconnection. We studied this case while considering wind as usual without any frequency response capabilities as well as by allowing wind to have combinations of inertial and PFR response capabilities. The following frequency metrics were used to evaluate the frequency response of an interconnection:

1. Initial rate of decline of frequency
2. Value of frequency nadir (Point C)
3. Transition time between the beginning of the disturbance and the frequency nadir (transition time from Point A to Point C)
4. Value of settling frequency (Point B)
5. Transition time between the frequency nadir and the settling frequency (transition time from Point C to B).

According to [14], many of the comments used to calculate the Interconnection Frequency Response Obligation (IFRO) are from statistical observations of events similar to the one shown in Figure 2. Various parameters—including the starting frequency, first step of UFLS, contingency criteria, withdrawal adjustment, ratio of the frequency value at Point C to the value at Point B (CB_R), and demand response credit—are used in the IFRO calculations. For the Western Interconnection, BAL-003-1 requires IFRO = -840 MW/0.1 Hz [14].

III. BASE CASE DEVELOPMENT AND MODELING ASSUMPTIONS

A. Base Case

The purpose of this study was to investigate the overall frequency response of the Western Interconnection with different levels of variable wind generation with enabled inertial and PFR controls using General Electric’s (GE’s) Positive Sequence Load Flow (PSLF) dynamic simulation software. For this purpose, we used one of the PSLF base cases developed under guidance by the Western Electricity Coordinating Council’s (WECC’s) Transmission Expansion Planning Policy Committee (TEPPC). In particular, the TEPPC 2022 light spring load base case (model 22lsp1s) [28], with approximately 15% instantaneous wind penetration, was selected as a basis for simulating future penetration scenarios. This particular base case under light spring load conditions throughout is consistent with 2022 U.S. state renewable portfolio standard requirements. Generation, load, and transmission topology were based on conditions modeled in the TEPPC 2022 common case [21].

Note that this modeling study did not address any changes to the limits of transmission lines that will take place at higher penetration levels. Instead, we adopted an approach of replacing the existing conventional power plants with wind power plants to achieve the desired penetration levels without transmission upgrades. At the snapshots of time represented in these cases for different penetration levels, the portion of generation coming from wind was in accordance with the results of the Western Wind and Solar Integration Study Phase 1 (WWSIS-1) [20]. WWSIS-1 looked at three different wind and photovoltaic scenarios to reach 30% penetration across the Western Interconnection footprint. For this study, we based the wind power location assumptions on an “In-area scenario,” in which each state meets its target using best in-state resources; thus, no additional interstate transmission was needed. The other two WWSIS-1 scenarios (“Local priority” and “Mega project”) required different levels of interstate transmission. In addition, the “Mega project” scenario located most of the wind power in a few very good wind resource areas, which caused localized frequency response from wind.

The breakdown of wind generation by turbine types for the TEPPC 2022 base case (15% penetration) is shown in Table I.

TABLE I. WWSIS-1 IN-AREA SCENARIOS

Wind Turbine Model	Total Nameplate Rating (GW)	Current Output (GW)
Type 1 (wt1g)	0.533	0.426
Type 2 (wt2g)	1.52	1.48
Type 3 Generic (wt3g)	5.436	4.146
Type 4 Generic (wt4g)	15.640	8.632
Type 3 and Type 4 GE Model (gewtg)	4.944	3.238

The 15% base case for this study was developed from the TEPPC 2022 base case by replacing all Type 3 and Type 4 generic models with GE dynamic models for doubly-fed induction generators and full-size, power converter-based wind turbines as implemented in GE’s PSLF dynamic simulation program [9]. These models were developed and validated specifically for the latest GE wind turbine generators and include inertial control schemes and active power control emulators for PFR. The Type 1 and Type 2 wind power plants were not replaced by the GE dynamic model, so a small amount of Type 1 and Type 2 wind turbine generators were still present in all simulated cases. They do not contribute to system PFR, but they provide direct inertial response. Overall, the base case has the same wind power penetration level as the original TEPPC case.

Other penetration level scenarios were developed based on the base case using the following guidance.

B. Scenario Development

The scenarios for this study were developed for five more penetration cases using (1) to replace conventional power plants with wind power plants:

$$\text{Total Wind Capacity} = \text{Penetration\%} \times \text{WECC Total Load (MW)} / 0.56 (1)$$

This rule is based on an average 56% capacity factor for wind power. This capacity assumption was based on an evaluation of wind speed resource data sets in WWSIS-1 for spring months (March through May).

In particular, during spring nighttime hours, approximately 70% of the time the wind speed was below 10 m/s. After detailed analysis of these wind speed data sets, a 56% capacity factor was selected for all wind generation in the Western Interconnection. This approach was different from the redispatch methodology used in [4], which implemented the 2/3–1/3 rule, which means that for every 3 MW of additional wind production, there is a 2-MW reduction in thermal unit commitment and a 1-MW reduction in thermal unit dispatch. This rule was based on the Multi-Area Production Simulation (MAPS) modeling used in [20].

In this study, we adopted a simplified approach because the units' locations were not as critical for understanding system frequency response in an interconnection. This approach is a simplistic way of emulating the forthcoming retirement of steam units because of U.S. Environmental Protection Agency regulations.

The total light spring load in the TEPPC 2022 base case is approximately 113 GW, so the total wind nameplate capacities for each penetration case used in this study could be calculated using (1). Table II shows the nameplate capacities and generation level by wind for each penetration case. The rest of the generation fleet has a total output of 166 GW in the 15% base case.

TABLE II. WIND NAMEPLATE CAPACITIES AND CURRENT GENERATION LEVELS

Wind Penetration Case	Total Wind Nameplate Capacity (GW)	Wind Generation Level (GW)
15% base case	23	17.92
20%	41.65	22.5
30%	60.34	33.76
40%	80.45	45.19
50%	101.67	56.89
80%	180.49	85.51

Table III shows the rated wind capacity installed in each state for penetration levels of 10%, 20%, and 30% in accordance with WWSIS-1. These numbers were used as a guideline to develop penetration scenarios for this study, especially to decide which conventional generators should be replaced by wind generators. WWSIS-1 cases also included 1.4 GW of concentrating solar power (CSP) with storage and 4.2 GW of solar photovoltaic that were not set to provide frequency response (except for the mechanical inertia of CSP plant generators).

The selection of conventional thermal units that were displaced by wind power plants was based on the approach to put new wind power plants at existing, large, fossil-fueled (steam) unit plants. During this high-wind spring period, these wind power plants would operate within the range from 50% to 60% of rated capacity. This approach gives an approximate but reasonable distribution of loadings on the wind power plants in WECC.

Additional details on the development of a base case for this study are described in [18], with the simulations

performed to investigate the sensitivity of various active power control parameters of wind generation on the performance metrics discussed above. In particular, the sensitivities to wind power providing only PFR or only inertial controls were investigated at penetration levels of 20%, 30%, and 40%. In this work, we presented cases with combined inertial and PFR response by wind power for two more wind penetration levels: 50% and 80%.

TABLE III. WWSIS-1 IN-AREA SCENARIOS

Wind Rating (MW), 10% Case	Wind Rating (MW), 20% Case	Wind Rating (MW), 30% Case
33,240	42,900	75,390

All simulations were conducted using the PSLF simulation tool. UFLS schemes in the model were disabled to show how far below these settings they still reach when scenarios would have triggered UFLS. Each interconnection had a target resource contingency protection criteria based on the largest N-2 loss-of-resource event [23]. For the Western Interconnection, that would be the loss of the two largest generating units in the Palo Verde nuclear facility, totaling 2,625 MW [23].

The combined inertial constant of rotating electrical machines that are directly coupled with the grid in the Western Interconnection for the base case is $H=5.3$ s. The value of H will decrease with each wind penetration level due to a decreased number of committed synchronous units.

A wind turbine must operate in curtailed mode to provide enough reserve for PFR response during underfrequency conditions. During normal operating conditions with near-nominal system frequency, the control is set to provide a specified margin by generating less power than is available from the unit. The reserve available (i.e., headroom) is the available power curtailed, which is shown as the reserve between the operational point and P_0 in Figure 3. Figure 3 also shows that a nonsymmetric droop curve is possible with wind power depending on system needs.

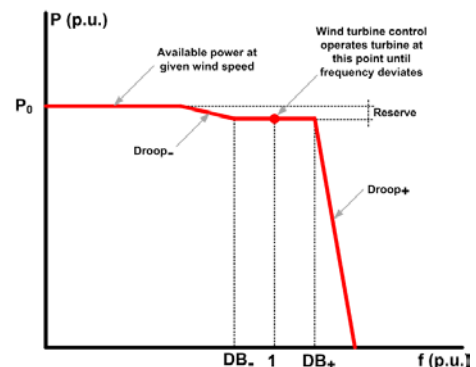


Figure 3. Wind power droop

Inertial control provides an inertial response capability for wind turbines—emulating the inertial response from conventional synchronous generators—for large underfrequency events. The response is provided by temporarily increasing the power output of the wind turbines in the range from 5% to 10% of the rated turbine power by extracting the inertial energy stored in the rotating masses. This short, quick power injection can benefit the grid by essentially limiting the rate of change of frequency at the

inception of the load/generation imbalance event. Figure 4 shows the measured frequency response of a 1.5-MW wind turbine generator triggered by the exact same frequency profile under different and highly turbulent wind speed conditions (tests conducted by NREL). The profile of each individual response is highly dependent on the initial turbine conditions (wind speed, power level, rotational speed) at the beginning of the underfrequency event and also the wind speed during the event.

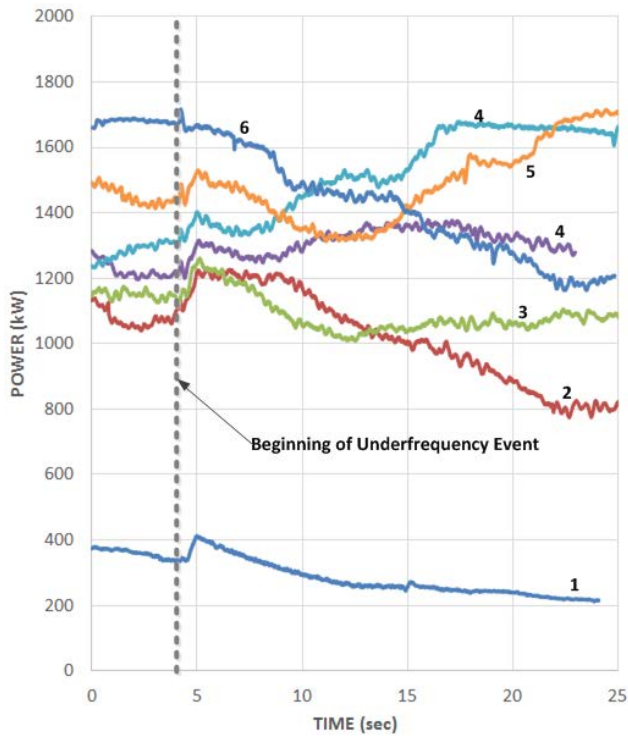


Figure 4. Examples of inertial response by 1.5-MW wind turbine generator

Figure 4 shows that the turbine under test consistently produced a short-term increase in power production at different power levels (traces 1-5). Subsequently, the turbine’s production decreased briefly due to the wind rotor deceleration. However, the level of the decline and the speed of the recovery depends on the wind speed conditions.

IV. SIMULATION RESULTS

Table IV provides a summary of the simulations performed to investigate the sensitivity of various active power control parameters of wind generation on the performance metrics discussed above. For each simulated case, the grid frequency was calculated at 10 key 500-kV buses in the Western Interconnection. For visual clarity, only the average of 10 frequencies is shown in the plots.

TABLE IV. SIMULATIONS PERFORMED

Case	Simulation Scenarios			
15%	No inertia, no PFR	Inertia only	PFR only (5% headroom; 4% droop)	Inertia + PFR (5% headroom; 4% droop)
20%				
30%				
40%				
50%				
80%				

A. Impact of Wind Power Penetration Levels and Active Power Control Strategies on Frequency Response

Figure 5–Figure 10 show the simulated frequency response for five instantaneous wind power penetration levels (15%, 20%, 30%, 40%, 50%, and 80%, respectively) and different active power control strategies from the wind power fleet. The increase in wind penetration had a visible impact on the performance metrics. The frequency nadir and settling frequency decline with penetration levels for the base case (blue plots) was caused by the lack of response from wind power replacing the responsive conventional generation.

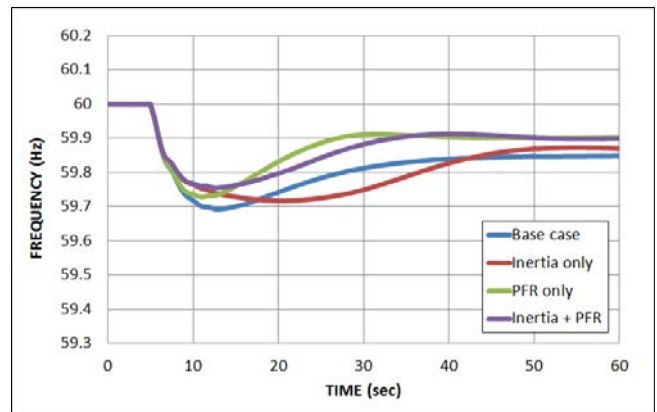


Figure 5. Western Interconnection frequency response for 15% wind penetration

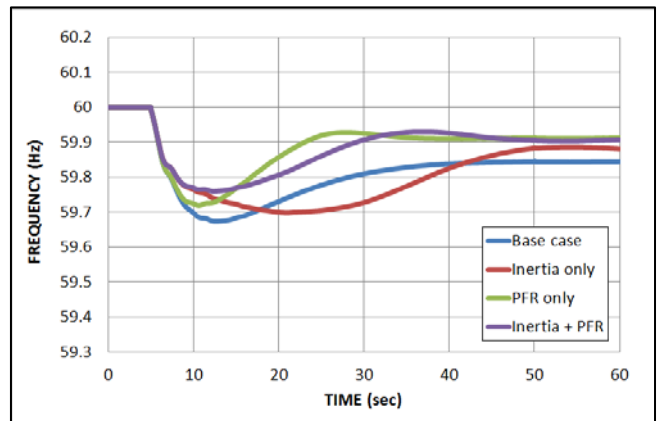


Figure 6. Western Interconnection frequency response for 20% wind penetration

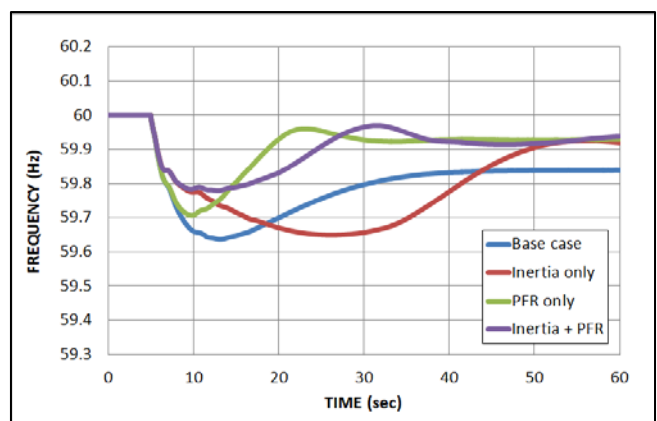


Figure 7. Western Interconnection frequency response for 30% wind penetration

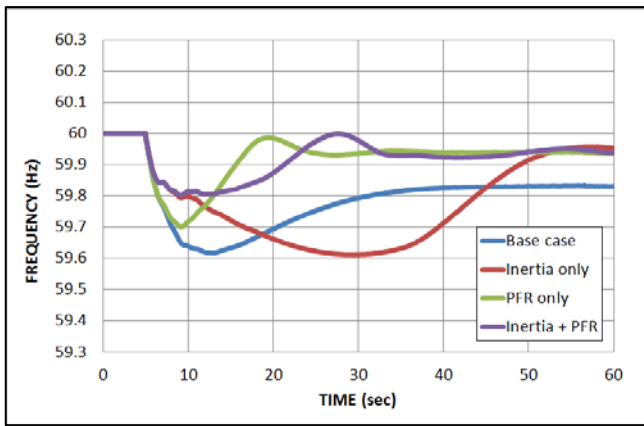


Figure 8. Western Interconnection frequency response for 40% wind penetration

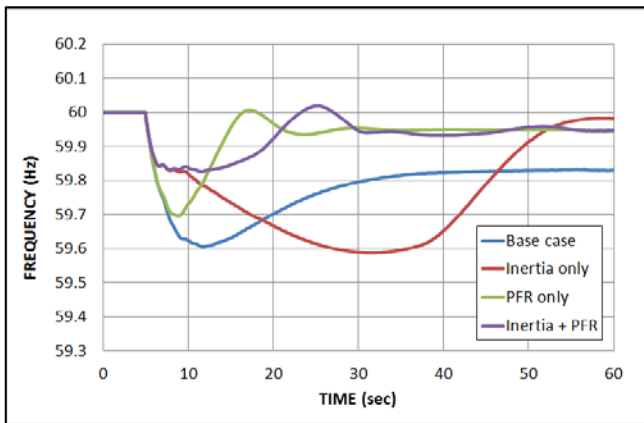


Figure 9. Western Interconnection frequency response for 50% wind penetration

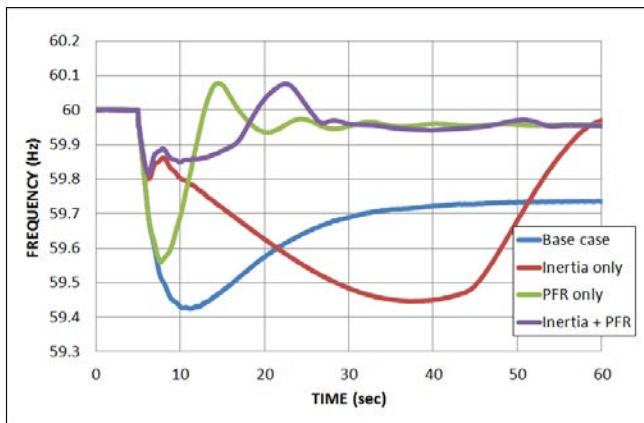


Figure 10. Western Interconnection frequency response for 80% wind penetration

Further analysis of Figure 5–Figure 10 revealed the impact of different active power control strategies. For lower penetration levels, the inertial control by wind (red trace) showed marginal improvement in the frequency nadir compared to the base case (Figure 5–Figure 7). At higher penetration levels, the frequency nadir was essentially the same as that of the base case at 40% penetration (Figure 8) and lower than the base case at 50% penetration (Figure 9). In the extremely high 80% penetration case, the frequency nadir was below the first UFLS stage at 59.5 Hz for both the base case and inertia-only case. Also, the nadir transition time increased with increasing penetration levels. This is because inertial control alone helped reduce only the initial

rate of decline of the frequency, which came at the expense of slowing down the wind rotors. Because of this slowdown, the wind turbines departed from their maximum power point, thus creating a deficiency of active power (the period of underproduction relative to the initial pre-fault operating point), and this resulted in a slower frequency recovery time. In addition, as shown in Figure 5–Figure 10, the recovery process was accompanied with overshoots, and it took longer to settle at a steady-state frequency (i.e., there was a longer transition to Point B).

On the other hand, enabling PFR created visible improvements in the frequency response, resulting in a better nadir and higher steady-state frequency, as shown in Figure 5–Figure 10 (green trace). Because of the same 5% headroom in all of the simulation scenarios, the frequency nadir of the PFR-only case did not change significantly with penetration level; however, it was consistently higher than the base case nadir for all penetration cases. The recovery of frequency was almost as fast as it was in the base case, with some oscillatory behavior depending on the penetration level. The biggest improvement was in the settling frequency level, which in the 80% case increased from 59.72 to 59.95.

As shown in Figure 5–Figure 10, combining inertial and PFR controls gave the most superior performance (magenta trace). This control strategy resulted in a largely higher frequency nadir with a somewhat slower recovery time than that of the PFR-only case.

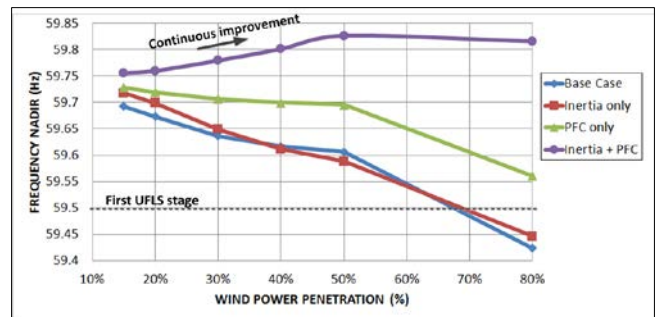


Figure 11. Impact of wind controls on frequency nadir

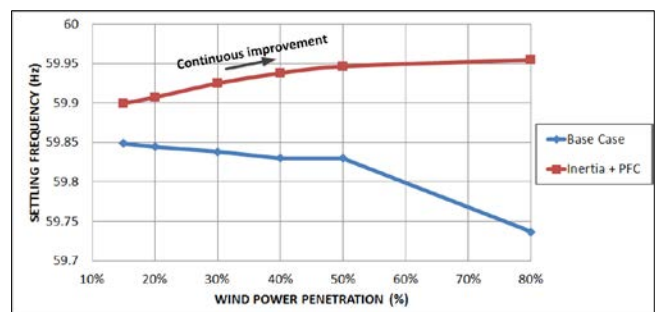


Figure 12. Impact of wind controls on settling frequency

The results of the simulations were consolidated in Figure 11, which shows the impact on frequency nadir for all penetration levels and wind power control strategies. Combining inertial and PFR controls for wind power resulted in a frequency nadir that was constantly increasing with penetration level (magenta trace) and had the best nadir performance at any wind penetration level than other control strategies. Another conclusion shown in Figure 11 (as mentioned earlier) is that providing inertial control only did

not give sufficient improvements compared to the base case. In fact, at penetrations greater than 30%, the inertial control resulted in a lower frequency nadir compared to the base case.

Despite the large decline in the frequency nadir for the base case, as wind penetration increased up to 50% (blue trace in Figure 11), it stayed above the highest UFLS setting of 59.5 Hz in the Western Interconnection after the loss of two Palo Verde units. It can be interpolated from Figure 11 that the UFLS setting was achieved at approximately 65% penetration. The highest wind penetration level of 80% resulted in a frequency nadir that was approximately 0.05 Hz below the UFLS setting. This suggests that frequency response in the Western Interconnection is not going to be in a major crisis—at least until extremely high penetrations are present; however, it is conceivable that some extreme conditions that were not envisioned in the study may result in unsatisfactory performance. In this regard, the advanced controls by wind power can help provide improved frequency response and reliability of the power system.

The impact of wind control on settling frequency is shown in Figure 12. The combination of inertial and PFR controls resulted in significant improvements of the settling frequency at all penetration levels. Similar to the frequency nadir, the settling frequency also increased with penetration level when wind provided control. The frequency response of the Western Interconnection was calculated from these settling frequencies, as shown in Table V. Both the MW/0.1 Hz and CB_R metrics showed sufficient improvements in the overall frequency response of the Western Interconnection. Note, again, that both metrics improved with penetration level when wind provided a combination of inertial and PFR response during a contingency event.

TABLE V. IMPACT OF WESTERN INTERCONNECTION FREQUENCY RESPONSE

Case	Base Case		Inertia + PFR	
	MW/0.1Hz	CB_R	MW/0.1Hz	CB_R
15%	1737	2.035	2616	2.439
20%	1690	2.105	2830	2.592
30%	1623	2.250	3500	2.944
40%	1546	2.259	4232	3.208
50%	1544	2.317	4908	3.247
80%	996	2.185	5799	4.073

The impact of wind control strategies on the power output of the selected wind power plant is shown in Fig. 12. The active power magnitudes did not change significantly with penetration when wind power was providing only inertial response (red traces in Figure 13). It did change, however, for the cases when wind power was providing PFC or combined inertial and PFC response (green and magenta traces). In fact, the burden of the frequency response on individual wind power plants decreased with penetration level because the response was spread among a larger number of wind power plants that were online.

The active power controls by wind power will have a profound impact on the frequency response of conventional generation. Such an impact will become more obvious at higher penetration levels. The performance impact for a selected Western Interconnection combined-cycle unit during the same event is shown in Figure 14.

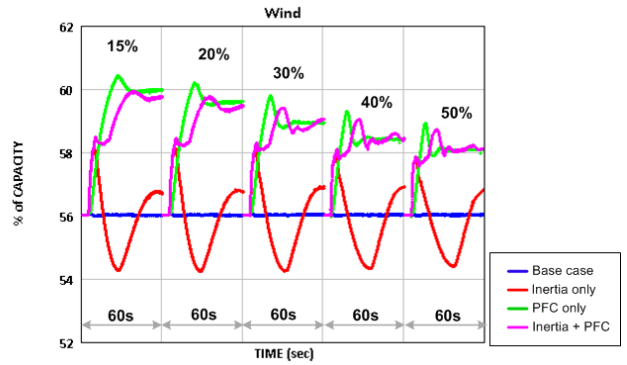


Figure 13. Impact of wind controls on wind power plants

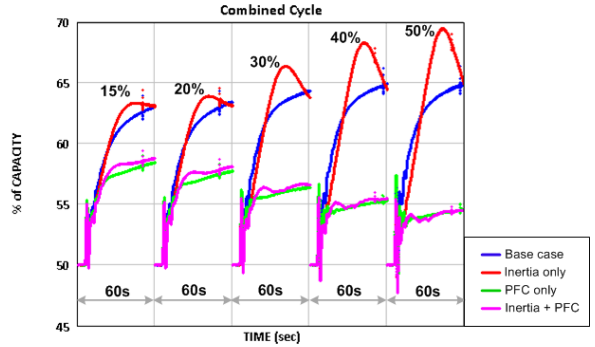


Figure 14. Impact of wind controls on conventional power plants

A closer look at Figure 14 reveals a significant reduction in the active power output of the selected combined-cycle units for the cases when wind power was providing only PFC or a combination of PFC and inertial controls. The power contribution from this unit increased with wind penetration level for a base case (blue trace) when all frequency response was provided by the conventional fleet. The magnitude of the power contribution by the conventional unit was higher when wind power was providing only inertial control (red trace). This was because all conventional units needed to provide additional energy to compensate for periods of underproduction by wind power caused by the deceleration of wind rotors; however, PFC and combined controls by wind significantly reduced the burden of frequency response by this combined-cycle unit, as shown in Figure 14 (green and magenta traces).

B. Impact of Wind Resource Diversity on Inertial Response

In previous sections, we described simulation cases in which all the wind power in the Western Interconnection was operating at below-rated wind speed. Such a simplification allows for a reasonable approximation of the overall frequency response at different penetration levels; however, actual wind conditions at individual power plants and even turbines will impact how they respond to frequency contingencies [15], [25]. In particular, the inertial response by wind power will be sensitive to the initial wind conditions during a contingency event. In this section, we took a first step toward simulating such diversity on the interconnection level in a dynamic study. We made the assumption that 10% of wind power in the whole Western Interconnection was operating in Region III (flat portion) of the power curve, whereas the remaining wind generation was still operating in Region II [26]. The 10% level was taken from an analysis of wind speeds on the Western

Interconnection during this season. Three cases were simulated to understand the impact of this diversity on the inertial response by wind for the 50% penetration case, as shown in Figure 15.

Case 1 represented a scenario in which all wind power in Region II provided only inertial response (the same as inertia only in Figure 9). Case 2 represented the scenario in which inertial response was provided by all wind power in the Western Interconnection when 10% of the wind power operated at above-rated wind speed. Case 3 represented a scenario in which the inertial response was provided by only 10% of the wind power operating at above-rated wind speed, with disabled inertial response in the rest of the wind power.

Figure 15 shows that the resulting frequency response with wind providing only inertial response was better in Case 2 than it was in Case 1 (with both a higher nadir and a faster recovery time). This is because the 10% of operating wind power produced a superior frequency response and faster recovery to the pre-fault operation point as a result of the available power in the wind. Case 3 demonstrated a poorer frequency nadir than Case 2 because less inertial power was produced by the wind generation, yet it was still superior to and performed better than the base case and Case 1.

The results of this section demonstrated the importance of more accurate representations of initial conditions at each wind power plant when providing inertial response on the interconnection level. It may lead system operators and wind power plant operators to better use the current information to determine whether synthetic inertial response will improve system reliability.

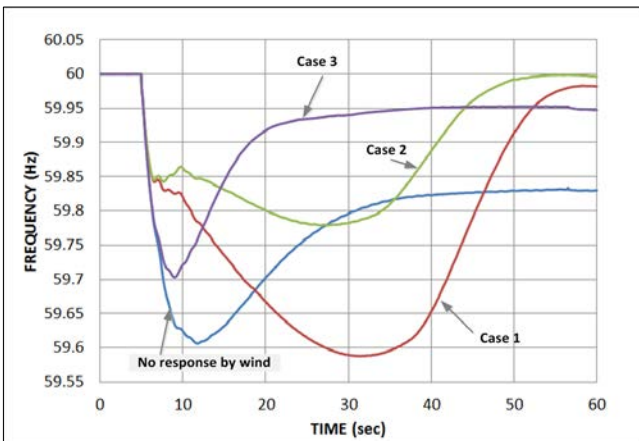


Figure 15. Impact of wind diversity on inertial response at 50% wind penetration

V. CONCLUSIONS

This simulation effort was conducted specifically to investigate the frequency response of the Western Interconnection caused by a large loss of generation and was not intended to address any stability-related impacts on transmission. Many factors and constraints (both technical and economic) affect the operation of a power system with high levels of wind generation. The depth of frequency excursions followed by a generation loss can be improved by inertial and/or PFR controls of variable-speed wind turbine generators. The industry is concerned about having inadequate frequency response in light of this changing generation mix as a result of the increasing penetration of

variable generation and planned retirements of fossil-fueled generation. Currently, the PFR from generation sources are not technology neutral. To consider all options toward improving the frequency performance, the industry needs to research, develop, and demonstrate newer and less familiar sources to provide frequency support.

The focus of the research presented in this paper was to assess the impact of different active power control strategies on the frequency response of an interconnection with a high level of wind penetration. We have investigated instantaneous wind penetrations as high as 80%, unveiling the system's vulnerability under these extremely high wind penetrations and possible mitigation strategies that wind can provide.

ACKNOWLEDGMENTS

This work was supported by the U.S. Department of Energy (DOE) under Contract No. DE-AC36-08GO28308 with NREL. Funding provided by the DOE Office of Energy Efficiency and Renewable Energy Wind Program. The authors would like to thank Charlton Clark of DOE for his continuous support of this work. The authors would also like to thank Dr. Erik Ela of the Electric Power Research Institute for his valuable guidance for this project.

REFERENCES

- [1] ENTSO-E, Operational Handbook Policy 1: Load-Frequency Control and Performance. Brussels, Belgium: Union for the Coordination of the Transmission of Electricity, March 2009.
- [2] Western Electricity Coordinating Council, "White paper on frequency responsive reserve standard," April 2005.
- [3] Joseph H. Eto et al., Use of Frequency Response Metrics to Assess the Planning and Operating Requirements for Reliable Integration of Variable Renewable Generation. Berkeley, CA: Ernest Orlando Lawrence Berkeley National Laboratory, Dec. 2010.
- [4] GE Energy, California ISO Frequency Response Study: Final Draft. Schenectady, NY: Nov. 9, 2011.
- [5] Eirgrid and SONI, All-island TSO Facilitation of Renewables Studies. Dublin, Ireland: June 2010.
- [6] North American Electric Reliability Corporation, "Industry Advisory: Reliability Risk—Interconnection Frequency Response (Revision 1). Washington, D.C.: Feb. 25, 2010.
- [7] J. Ingleson and E. Allen, "Tracking the Eastern Interconnection frequency governing characteristic" (paper presented at the 2010 IEEE PES GM, Minneapolis, MN).
- [8] "M-4 Interconnection Frequency Response," www.nerc.com.
- [9] N. W. Miller, M. Shao, S. Pakic, and R. D. Aquila, Western Wind and Solar Integration Study Phase 3—Frequency Response and Transient Stability. Golden, CO: Dec. 2014.
- [10] R. P. Schulz, "Modeling of governing response in the Eastern Interconnection" (paper presented at the 1999 IEEE PES Winter Meeting, New York, NY).
- [11] S. Virmani, "Security impacts of changes in governor response" (paper presented at the 1999 Proc. IEEE PES Winter Meeting, New York, NY).
- [12] T. Weissbach and E. Welfonder, "High-frequency deviations within the European power system: Origins and proposals for improvement" (paper presented at the 2009 Power Systems Conference and Exposition, Seattle, WA).
- [13] E. Ela, A. Tuohy, M. Milligan, B. Kirby, and D. Brooks, "Alternative approaches for a frequency responsive reserve ancillary service market," *The Electricity Journal*, vol. 25, no. 4, pp. 88–102, May 2012.
- [14] IEEE Task Force on Large Interconnected Power Systems Response to Generation Governing, "Interconnected power system response to generation governing: Present practice and outstanding concerns," IEEE Special Publication 07TP180, May 2007.

- [15] North American Electric Reliability Corporation, Frequency Response Initiative Report—The Reliability Role of Frequency Response. Washington, D.C., Oct. 2012.
- [16] Federal Energy Regulatory Commission, BAL-003-1—Frequency Response and Frequency Bias Setting. Washington, D.C.: March 2013.
- [17] N. W. Miller, K. Clark, and M. Shao, “Impact of frequency responsive wind plant controls on grid performance” (paper presented at the 9th Int. Workshop on Large-Scale Integration of Wind Power, Quebec, Canada, 2010).
- [18] I. Margaritis, S. Papathanassiou, N. Hatzargyriou, A. Hansen, and P. Sorensen, “Frequency control in autonomous power systems with high wind power penetration,” *IEEE Trans. on Sustainable Energy*, vol. 3, no. 2, April 2012.
- [19] N. Miller, M. Shao, S. Pajic, and R. D’Aquila, Eastern Frequency Response Study (NREL/SR-5500-58077). Golden, CO: National Renewable Energy Laboratory, May, 2013. <http://www.nrel.gov/docs/fy13osti/58077.pdf>.
- [20] V. Singhvi et al., “Impact of wind active power control strategies on frequency response of an interconnection,” (paper presented at the 2013 IEEE PES GM, Vancouver, Canada).
- [21] V. Gevorgian, Y. Zhang, and E. Ela, “Investigating the impacts of wind generation participation in interconnection frequency response,” *IEEE Trans. Sustain. Energy*, vol. 6, no. 3, 2015.
- [22] Y. C. Zhang, V. Gevorgian, E. Ela, V. Singhvi, and P. Pourbeik, “Role of wind power in primary frequency response of an interconnection” (paper presented at the Int. Workshop on Large-Scale Integration of Wind Power, London, Oct. 2013). <http://www.nrel.gov/docs/fy13osti/58995.pdf>.
- [23] GE Energy, Western Wind and Solar Integration Study (NREL/SR-550-47434). Golden, CO: National Renewable Energy Laboratory, May 2010. <http://www.nrel.gov/docs/fy10osti/47434.pdf>.
- [24] TSS base cases, <http://www.wecc.biz>.
- [25] K. Clark, N. Miller, and J. J. Sanchez-Gasca, Modeling of GE Wind Turbine-Generators for Grid Studies, V4.5. Schenectady, NY: GE Energy, 2008.
- [26] U.S. Energy Information Administration, 2011 Net Winter Ratings per Form EIA-860, 2011 data. <http://www.eia.gov/electricity/data/eia860>.
- [27] E. Ela, V. Gevorgian, A. Tuohy, B. Kirby, M. Milligan, and M. O’Malley, “Market designs for the primary frequency response ancillary service—Part I: Motivation and design,” *IEEE Trans. Power Syst.*, to be published.
- [28] E. Muljadi and C. Butterfield, “Pitch-controlled variable-speed wind turbine generation,” *IEEE Trans. Ind. App.*, vol. 37, no. 1, 2001.
- [29] K. Johnson, Adaptive Torque Control of Variable-Speed Wind Turbines (NREL/TP-500-36265). Golden, CO: National Renewable Energy Laboratory, Aug. 2004. <http://www.nrel.gov/docs/fy04osti/36265.pdf>.
- [30] P. Kundur, Power System Control and Stability: Electric Power Research Institute Power System Engineering Series. New York: McGraw-Hill Education, 1994.
- [31] Western Electricity Coordinating Council, “2022 Common Case Reliability Assessment of Light Spring Condition,” www.wecc.biz.